

# HEAT AND MASS TRANSFER IN 3D MHD WILLIAMSON-CASSON FLUIDS FLOW OVER A STRETCHING SURFACE WITH NON-UNIFORM HEAT SOURCE/SINK

*Chakravarthula S. K. RAJU<sup>1</sup>, Naramgari SANDEEP<sup>2</sup>, Mohamed E. ALI<sup>3\*</sup>, Abdullah O. NUHAI<sup>3</sup>*

<sup>1,2</sup>Department of Mathematics, VIT University, Vellore-632014, India., <sup>2</sup>[dr.nsrh@gmail.com](mailto:dr.nsrh@gmail.com)

<sup>3</sup>Mechanical Engineering Department, College of Engineering, King Saud University, P. O. Box 800, Riyadh 11421, Saudi Arabia.

\*Corresponding author Email: [mali@ksu.edu.sa](mailto:mali@ksu.edu.sa)

*A Mathematical model has been proposed for investigating the flow, heat and mass transfer in Williamson and Casson fluid flow over a stretching surface. For controlling the temperature and concentration fields we considered the space and temperature dependent heat source/sink and homogeneous-heterogeneous reactions respectively. Numerical results are carried out for this study by using Runge-Kutta based shooting technique. The effects of governing parameters on the flow, heat and mass transfer are illustrated graphically. Also computed the skin-friction coefficients for axial and transverse directions along with the local Nusselt number. In most of the studies, homogeneous-heterogeneous profiles were reduced into a single concentration equation by assuming **equal** diffusion coefficients. For the physical relevance, without any assumptions we studied the individual behavior of the homogeneous-heterogeneous profiles. It is found that the rate of heat and mass transfer in Casson fluid is significantly large while equated with the heat and mass transfer rate of Williamson fluid.*

**Keywords:** *MHD, non-Newtonian fluid, Stretching sheet, non-uniform heat source/sink, homogeneous-heterogeneous reactions.*

## 1. Introduction

The boundary layer flow, heat and mass transfer over a stretching surface has benefitted believed attention due to its demand in the industrial and manufacturing processes. Such demanded applications are of polymer, chemical industries, controlling of cooling and heating processes and blood flows. Due to this significance the innovation of the boundary layer flow past a stretching sheet was initiated by Sakiadis [1]. The study of flow through stretching sheet in the presence of chemical reaction place an important role in the chemical engineering, biomedical, pharmaceutical industries, polythene paper production and environmental engineering processes these were given by Ali and Al-Yousef [2]. Later on, the self-similarity solution of continuously stretched surfaces with decreasing velocities was discussed by Magyari et al. [3]. An analytical solution for MHD flow past a permeable vertical stretching surface with existing of chemical reaction was discussed by Chamka [4]. Raptis and Perdikis [5] analyzed the MHD two-dimensional viscous flow through a nonlinearly stretching sheet with existing of chemical reaction. The chemical reaction and heat generation effect on the flow through porous medium was illustrated by

Patil and Kulkarni [6]. Mixed convection on flow over a moving vertical surface in the presence of variable viscosity was analyzed by Ali [7]. The mass transfer analysis of MHD flow of a second grade fluid past a permeable stretching sheet in the presence of chemical reaction was studied by Cortell [8].

Past few decades heat and mass transfer in non-Newtonian fluid flows are playing a vital role than heat and mass transfer in Newtonian fluids due to its simplicity in nature. There are many practical real time, engineering applications of non-Newtonian fluids such as crystal growing, drilling mud's, gels, shampoos, powder technology, food processing, blood flow and biological applications. There are various types of non-Newtonian fluids like Casson, viscoelastic, Jeffrey and Williamson fluid. There is no constitutive relation for these fluids so these fluids have simplicity in nature. In the present study, we considered the Casson fluid, it is a shear thinning liquid having an infinite viscosity at rate of shear stress is zero. Owing to this Raju et al. [9] analyzed an unsteady Casson fluid flow through a stretching sheet in the presence of variable thermal conductivity. Haq et al. [10] studied the heat transfer characteristics of a Casson nano fluid flow past a shrinking sheet. An unsteady Casson fluid flow past an oscillating vertical plate was studied analytically by Hussain et al. [11]. Raju et al. [12] investigated the mass transfer analysis of MHD Casson fluid flow past a permeable exponentially stretching sheet. The Casson fluid flow past an exponentially shrinking surface was illustrated by Nadeem et al. [13]. Most of the above mentioned studies are belonging to two-dimensional, steady, unsteady, exponentially stretching sheets. The 3D flow of non-Newtonian fluids through a stretching surface also has most applications in the civil engineering, solar energy, and peristalsis blood flow through a pumps etc. Nadeem et al. [14] depicted the 3D flow of Casson nanofluid through a linear stretching surface. Couple stress fluid flow through a stretching sheet in the presence of Newtonian heating effect was discussed by Ramezan et al. [15]. Hayat et al. [16] depicted the radiation effect on 3D Jeffrey fluid flow past a stretching surface in the presence of variable thermal conductivity. The natural convection flow induced by a continuous stretched sheets in the presence of rapidly depreciating velocities Ali [17].

The magnetohydrodynamic flows with non-uniform heat source/sink also plays major in the fields of aerodynamics, aeronautical engineering, astrophysics, space technology and environmental engineering etc. The Williamson fluid flow past a stretching sheet also have vital role in the field of plasma dynamics, blood flows, ice slurries, ice creams, paste, oil crude preparation, petroleum engineering sandwich processes and bio thermal engineering etc. In modern technology, the researchers are interested into the Williamson fluid flow through a stretching sheet due to its applications in blood flows; these were addressed by researchers [18-23]. Hayat et al. [24] explored the convective conditions on peristaltic flow with homogeneous-heterogeneous reactions. Homogeneous-heterogeneous reaction effect on stagnation-point flow past a stretching surface was illustrated by Bachok et al. [25]. Chatterjee [26] studied the steady axisymmetric Carreau fluid jet flow through an impinging surface. Viscoelastic fluid flow past a saturated porous medium was analyzed by Delenda et al. [27]. The researchers [31-38] analyzed the flow over various geometries (cone, plate and sheet) with various flow physical characteristics (non-uniform heat source or sink, Nano liquids and magnetic field).

All the above mentioned studies concentrated on 2D or 3D flows in the presence of chemical reaction, magnetic field and radiation. But no studies have been described yet up to the author's knowledge on the flow of 3D non-Newtonian fluids over a stretching surface in the presence of non-

uniform heat source/sink and homogeneous-heterogeneous reactions. By keeping this into view in this study we make an attempt to analyze the heat and mass transfer behavior of the three-dimensional Casson and Williamson fluid flows through a stretching sheet with non-uniform heat source/sink and homogeneous-heterogeneous reactions.

## 2. Flow analysis

In this study we consider the electrically conducting Casson and Williamson fluid flows past a stretching sheet in the presence of magnetic field, non-uniform heat source/sink and homogeneous-heterogeneous reactions. The magnetic Reynolds is negligible in this study. Due to this cause we neglected the induced magnetic field. The mass transport was controlling by homogeneous and heterogeneous reactions. The flow configuration is displayed in Fig.1. The rheological model for an isotropic flow of Casson fluid is given by Raju and Sandeep [39]:

$$\tau^{1/n} = \tau_0^{1/n} + \mu \dot{\gamma}^{1/n} \quad (1)$$

$$\tau_{i,j} = \begin{cases} 2(\mu_B + p_y / \sqrt{2\pi}) e_{ij}, \pi \succ \pi_c \\ 2(\mu_B + p_y / \sqrt{2\pi}) e_{ij}, \pi \prec \pi_c \end{cases} \quad (2)$$

In the above equation  $\pi = e_{ij}e_{ij}$  and  $e_{ij}$  is the  $(i, j)$  th component of the deformation rate,  $\pi$  the product of the component of deformation rate with itself,  $\pi_c$  is a critical value of this product based on the non-Newtonian model,  $\pi_B$  is the plastic dynamic viscosity of non-Newtonian fluid, and  $p_y$  is the yield stress of the fluid. The anonymous researchers has suggested the value of  $n=1$ . However, in many applications this value is  $n > 1$ .

Similarly, the constitutive equation for Williamson fluid model is given by (Nadeem et al. [40])

$$S = -pI + \tau \quad (3)$$

$$\tau = \left[ \mu_\infty + \frac{\mu_0 - \mu_\infty}{1 - \Gamma \dot{\gamma}} \right] A_1 \quad (4)$$

Here  $p$  is the pressure  $I$  is identity vector,  $\tau$  is the extra stress tensor  $\mu_0$  and  $\mu_\infty$  are the limiting viscosities at zero and infinite shear rate.  $\Gamma > 0$  is the time constant,  $A_1$  is the first Rivlin Ericksen tensor and  $\dot{\gamma}$  is defined as

$$\dot{\gamma} = \sqrt{1/2\pi}, \pi = \text{trace}(A_1^2) \quad (5)$$

Here we have only considered the case for which  $\mu_\infty=0$  and  $\Gamma \dot{\gamma} < 1$ . Thus, extra stress tensor takes the form as

$$\tau = \left[ \frac{\mu_0}{1 - \Gamma \dot{\gamma}} \right] A_1 \quad (6)$$

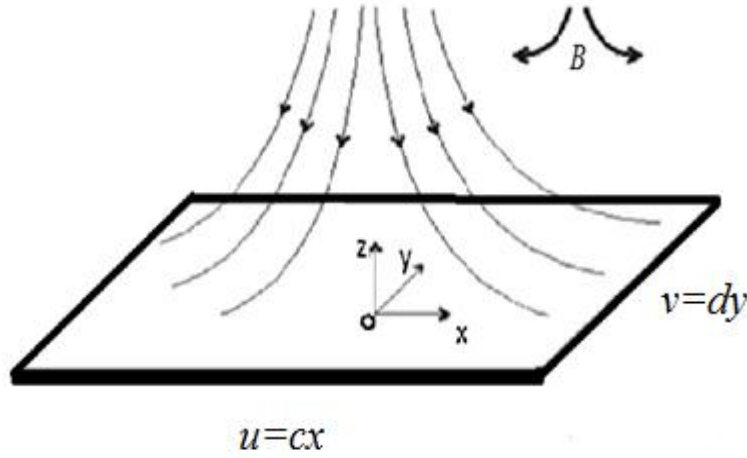


**Fig.1 Flow Configuration**

In this study we combined the Casson and Williamson and based on assumptions the governing boundary layer equations are given by (Haq et al. [10], Nadeem et al. [13], Raju and Sandeep [39])

$$\frac{\partial u}{\partial x} + \frac{\partial v}{\partial y} + \frac{\partial w}{\partial z} = 0, \quad (7)$$

$$\left( u \frac{\partial u}{\partial x} + v \frac{\partial u}{\partial y} + w \frac{\partial u}{\partial z} \right) = \nu \left( 1 + \frac{1}{\beta} \right) \frac{\partial^2 u}{\partial z^2} - \frac{\sigma B_0^2}{\rho} u + \sqrt{2\Gamma} \frac{\partial u}{\partial z} \frac{\partial^2 u}{\partial z^2}, \quad (8)$$

$$\left( u \frac{\partial v}{\partial x} + v \frac{\partial v}{\partial y} + w \frac{\partial v}{\partial z} \right) = \nu \left( 1 + \frac{1}{\beta} \right) \frac{\partial^2 v}{\partial z^2} - \frac{\sigma B_0^2}{\rho} v + \sqrt{2\Gamma} \frac{\partial v}{\partial z} \frac{\partial^2 v}{\partial z^2}, \quad (9)$$

The corresponding boundary conditions are:

$$\begin{aligned} u = u_w(x) = cx, v = v_w(y) = dy, w = 0, \text{ at } z = 0, \\ u \rightarrow 0, v \rightarrow 0, w \rightarrow 0, \quad \text{ at } z = \infty, \end{aligned} \quad (10)$$

In the above equations  $\beta \rightarrow \infty$ ,  $\Gamma \neq 0$  is called Williamson fluid and  $\beta \neq 0$ ,  $\Gamma = 0$  is called Casson fluid. To convert the governing equations into set of nonlinear ordinary differential equations, we now introduce the following similarity transformation.

$$u = cxf'(\eta), v = dyg'(\eta), w = -(c\nu)^{0.5} (f(\eta) + g(\eta)), \eta = \nu_f^{-0.5} c^{0.5} z, \quad (11)$$

The Equations (4) and (5) are substitute into equation (1)-(3) we get newly coupled transformed nonlinear equation, which are given by,

$$\left(1 + \frac{1}{\beta}\right) f''' + \lambda f' f''' - M f' + (f + g) f'' - f'^2 = 0, \quad (12)$$

$$\left(1 + \frac{1}{\beta}\right) g''' + \lambda g' g''' - M g' + (f + g) g'' - g'^2 = 0, \quad (13)$$

The transformed boundary conditions are:

$$\begin{aligned} f = 0, g = 0, f' = 1, g' = 1, \quad \text{at } \eta = 0, \\ f' = 0, g' = 0, \quad \text{at } \eta \rightarrow \infty, \end{aligned} \quad (14)$$

where  $\beta$  is Casson parameter,  $\lambda$  is Non-Newtonian Williamson fluid parameter,  $M$  is magnetic field parameter, which are given by

$$\lambda = \Gamma x \sqrt{2c^3 / \nu}, M = \sigma B_0^2 / \rho c,$$

For engineering interest physical quantities are the shear stress coefficients  $C_{fx}, C_{fy}$  (friction factors) are given by

$$\text{Re}_x^{1/2} C_{fx} = \left(1 + \frac{1}{\beta}\right) \lambda f''(0), \text{Re}_x^{1/2} C_{fy} = \left(1 + \frac{1}{\beta}\right) \lambda g''(0), \quad (15)$$

### 3. Heat Transfer Analysis

The energy equation with non-uniform heat source or sink is given by

$$\left(u \frac{\partial T}{\partial x} + v \frac{\partial T}{\partial y} + w \frac{\partial T}{\partial z}\right) = \alpha \frac{\partial^2 T}{\partial z^2} + \frac{1}{\rho c_p} q''', \quad (16)$$

The boundary conditions for the energy equation is given by

$$T = T_w, \quad \text{at } z = 0, \quad T = T_\infty, \quad \text{as } z \rightarrow \infty, \quad (17)$$

The time dependent non-uniform heat source/sink  $q'''$  is defined as

$$q''' = \frac{ku_w(x)}{x\nu} \left(A^*(T_w - T_\infty) f' + B^*(T - T_\infty)\right), \quad (18)$$

in the above equation positive values of  $A^*, B^*$  correspond to heat generation and negative values are correspond to heat absorption. We define a dimensionless parameter for temperature variable  $\theta(\eta)$  of the form

$$\theta(\eta) = \frac{T - T_\infty}{T_w - T_\infty}, \quad (19)$$

Substituting equation (13) into equations (10)-(12) we get the transformed non-dimensional temperature equation as given by,

$$\theta'' + \text{Pr}(f + g)\theta' + A^* f' + B^* \theta = 0, \quad (20)$$

With the transformed boundary conditions

$$\theta = 1, \quad \text{at } \eta = 0, \quad \theta = 0, \quad \text{as } \eta \rightarrow \infty, \quad (21)$$

The local Nusselt number is defined by:

$$Nu_x = \frac{xq_w}{k_f(T_w - T_\infty)}, \quad \text{where } q_w = -k \left( \frac{\partial T}{\partial z} \right)_{z=0}, \quad (22)$$

$$\text{Re}_x^{-1/2} Nu_x = -\theta'(0), \quad (23)$$

#### 4. Mass Transfer Analysis

It is assumed that a simple homogeneous-heterogeneous reaction model exists as proposed by Chaudhary and Merkin [29] in the following form:

$$\left( u \frac{\partial a}{\partial x} + v \frac{\partial a}{\partial y} + w \frac{\partial a}{\partial z} \right) = D_A \frac{\partial^2 a}{\partial z^2} - k_c ab^2, \quad (24)$$

$$\left( u \frac{\partial b}{\partial x} + v \frac{\partial b}{\partial y} + w \frac{\partial b}{\partial z} \right) = D_B \frac{\partial^2 b}{\partial z^2} + k_c ab^2, \quad (25)$$

The respective boundary conditions are given by

$$D_A \frac{\partial a}{\partial z} = k_s a(z), D_B \frac{\partial b}{\partial z} = -k_s a(z) \quad \text{at } z = 0, \quad (26)$$

$$a(z) = a_0, b(z) = 0 \quad \text{as } z \rightarrow \infty,$$

Where  $a$ ,  $b$  are the concentrations of the chemical species,  $D_A$  and  $D_B$  are the diffusion coefficients,  $k_c$  and  $k_s$  are the rate constants. We now introduced the similarity transformations as

$$G(\eta) = a/a_0, H(\eta) = b/a_0, \quad (27)$$

By substituting equation (21) into equations (18) and (19) we get

$$G'' + Sc((f + g)G' - KGH^2) = 0, \quad (28)$$

$$\delta H'' + Sc((f + g)H' + KGH^2) = 0, \quad (29)$$

The transformed boundary conditions are

$$\begin{aligned} G' &= K_s G, \delta H' = -K_s G & \text{at } \eta = 0, \\ G &= 1, H = 0 & \text{as } \eta \rightarrow \infty, \end{aligned} \quad (30)$$

where  $Sc$  is the Schmidt number,  $K$  is the measure of strength of homogeneous reaction,  $K_s$  is the strength of heterogeneous reaction,  $Re = c/\nu$  is the Reynolds number and  $\delta$  is the ratio of diffusion coefficients, which are represented below.

$$\left. \begin{aligned} \delta &= \frac{D_B}{D_A}, Sc = \frac{\nu}{D_A}, K = \frac{k_c a_0^2}{c}, K_s = \frac{k_s}{D_A \sqrt{Re}} \end{aligned} \right\} \quad (31)$$

For physical quantities of engineering interest the local Sherwood number  $Sh_x$  is given by

$$Re_x^{-1/2} Sh_x = -\phi'(0), \quad (32)$$

### 5. Method of Solution

To solve the present problem, Eqs. (6), (7), (14), (22) and (23) with the corresponding boundary conditions (Eqs. (8), (15) and (24)) are transformed into a set of first order differential equations. Now, Runge-Kutta and Shooting technique is applied to develop the numerical code. In this methodology, the above mentioned nonlinear ODEs converted to a first order differential equation, by using the following method:

$$f' = y_2, f'' = y_3, g' = y_5, g'' = y_6, \theta = y_7, \theta' = y_8, G = y_9, G' = y_{10}, H = y_{11}, H' = y_{12} \quad (33)$$

$$f''' = \frac{1}{(1 + \lambda y_2 + (1/\beta))} (M y_2 + (y_1 + y_4) y_3 - y_2^2) \quad (34)$$

$$g''' = \frac{1}{(1 + \lambda y_2 + (1/\beta))} (M y_5 + (y_1 + y_4) y_5 - y_5^2) \quad (35)$$

$$\theta'' = -Pr((y_1 + y_4) y_8) - A^* y_2 - B^* y_7 \quad (36)$$

$$G'' = -Sc((y_1 + y_4) y_{10} + K y_9 y_1^2) \quad (37)$$

$$H'' = -Sc((y_1 + y_4) y_{12} + K y_9 y_1^2) \quad (38)$$

with boundary conditions are

$$\begin{aligned} y_1 = 0, y_2 = 1, y_4 = 0, y_5 = 1, y_7 = 1, y_{10} = K_s y_9, \delta y_{12} = -K_s y_9 & \text{ at } \eta \rightarrow 0 \\ y_2 = 0, y_5 = 0, y_7 = 0, y_9 = 1, y_{11} = 0 & \text{ at } \eta \rightarrow \infty \end{aligned} \quad (39)$$

Initially, the guess values of  $y_3(0), y_6(0), y_8(0)$ , are used in the simulation which are not given at the initial condition. In this study, the successive iteration length is 0.01. Firstly, the accuracy of the guess values  $y_3(0), y_6(0), y_8(0)$  is verified by comparing the estimated values of  $y_2(0), y_4(0), y_5(0), y_7(0)$  at  $\eta = \eta_{\max}$  using MATLAB software ode45 solver. Finally, the Runge-

Kutta fourth order method is used to integrate the Eqs. (28)- (32) and the iteration continued until the agreement between the estimated values and given condition at  $\eta = \eta_{\max}$ . It is found that a grid size of 300 ensure the grid independent solution for the present case. The accuracy of the present numerical simulation results are validated with the previous study of Ahmad and Nazar [30] (see, Table 3) and found excellent agreement with their results.

## 6. Results and Discussion

The non-dimensional governing equations (6), (7), (14), (22) and (23) subject to the respective boundary conditions (8), (15) and (24) are solved numerically using Runge-Kutta based shooting technique Sandeep and Sulochana [28]. Results depict the influence of the dimensionless physical governing parameters on the flow, heat and mass transfer in Casson and Williamson fluids. For numerical computations we considered the non-dimensional values as  $A^* = B^* = 0.1$ ,  $Sc = K_s = K = \delta = 1$ ,  $Pr = 2$ ,  $M = \beta = 0.5$ . These values are kept as common in the entire study except the varied values are shown in respective figures and tables.

Figs. 2-6 depict the effect of magneticfield on the flow velocity, temperature and concentration fields. It is evident that for higher values of magneticfield parameter we noticed fall in the velocity and homogeneous concentration field. An opposite results have been observed for temperature and heterogenous field. This is due to the well-known fact that growth in the magneticfield develops the drag forces opposite to the flow. These forces produce the temperature near the surface. Due to this sense we had seen a raise in the temperature and depreciation in the velocity field. But due to the small variations in the temperature field we have noticed a mixed performance in the concentration profiles. It is evident to conclude that while compared with the Williamsons fluid, the momentum, concentration and temperature profiles of Casson fluid is highly influenced by the magneticfield parameter.

Figs.7 and 8 elucidates the effect of strength of heterogeneous parameter on concentration field. With an increment in the heterogeneous parameter we have perceived a fall in the homogeneous concentration profiles and a growth in the heterogeneous concentration field. It also observed that the influence of heterogeneous parameter is highly significant in Casson fluid. Because the concentration boundary layer thickness of a Casson fluid is gradually increases for smaller variations in the strength of heterogeneous parameter. Similar types of results have been observed with an increase in the strength of homogeneous parameter, these are displayed in Figs. 9 and 10.

The influence of  $A^*$  and  $B^*$  on temperature field is displayed in Figs. 11 and 12. It is evident that an increase in the space-dependent and temperature-dependent heat source/sink leads to enhance the temperature profiles throughout the boundary layer. This agrees with the general fact that the positive values of  $A^*$  and  $B^*$  acts like heat generators. Generating the heat means releasing the heat energy to the flow, these causes to boost up the thermal boundary layer thickness. It is interesting to note that the heat transfer production of the Casson fluid is comparatively better than the heat transfer production of the Williamsons fluid due to an increase in the non-uniform heat source/sink parameters.

Tables 1 depict the effects of non-dimensional principal parameters on skin-friction coefficients for axial and transverse directions for both Williamson and Casson fluids. It noticed that a rise in the values of magneticfield and porosity parameters reduces the friction factors for both Williamson and



Casson fluids. An increase in homogeneous-heterogeneous reactions does not shown significant variation in the friction factors. Table 2 shows the variation in the local Nusselt number due to the change in governing physical parameters. It is clear that an increase in the magneticfield, porosity and non-uniform heat source/sink parameters reduces the heat transfer rate. Table 3 illustrates the effects of non-dimensional governing parameters on homogeneous-heterogeneous mass transfer rate. It is visible from that magnetic field parameter have tendency to enhances the homogeneous mass transfer rate and depreciates the heterogeneous mass transfer rate. We have seen a similar type of results with an increase in the homogeneous reaction parameter. But a raise in the heterogeneous parameter suppresses the mass transfer rate. Table 4 shows the validation of the present results with the existed literature. We found an excellent agreement of the present results with the published work.

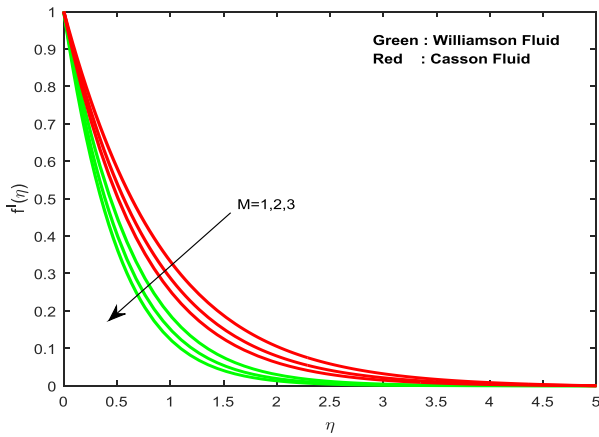


**Fig.2 Velocity field for different values of magnetic parameter**

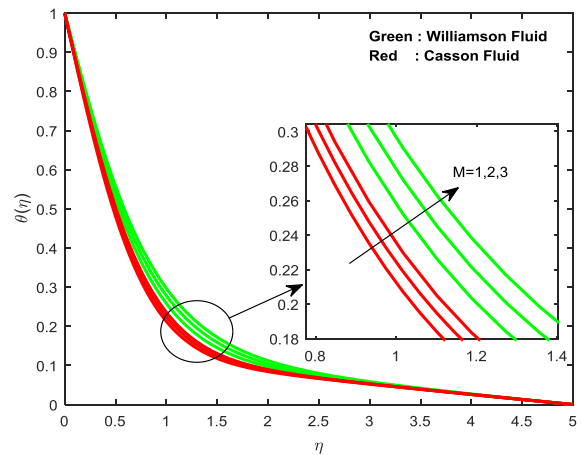


**Fig.4 Temperature field for different values of magnetic parameter**

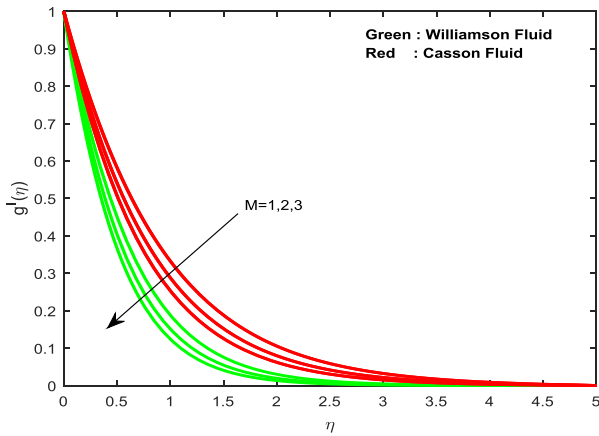


**Fig.3 Velocity field for different values of magnetic parameter**

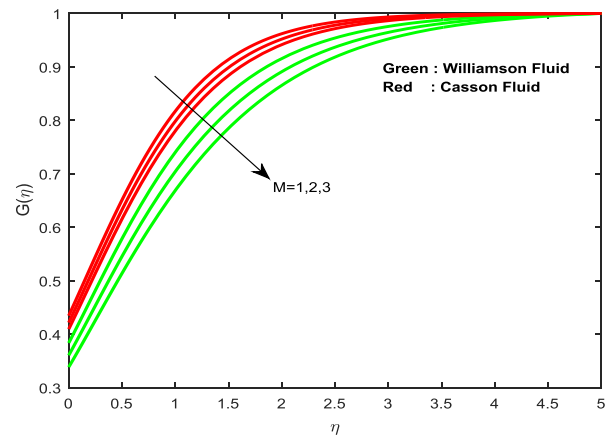


**Fig.5 Concentration field for different values of magnetic parameter**

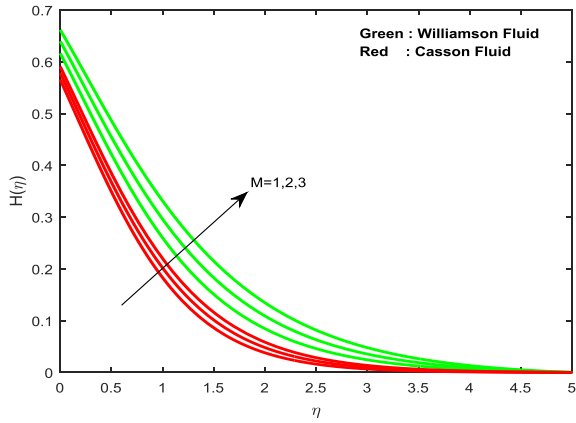


**Fig.6** Concentration field for different values of magnetic parameter

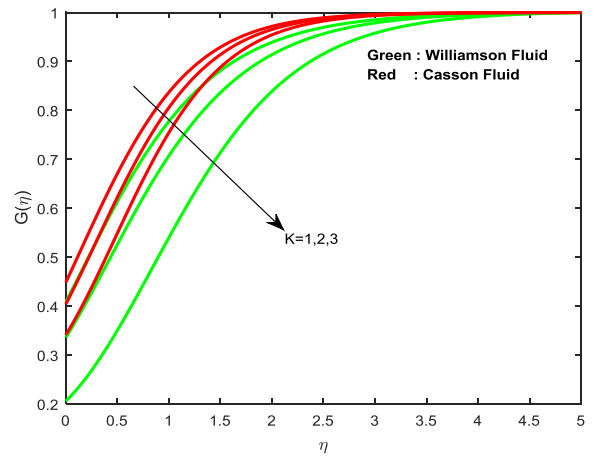


**Fig.9** Concentration field for different values of homogeneous parameter

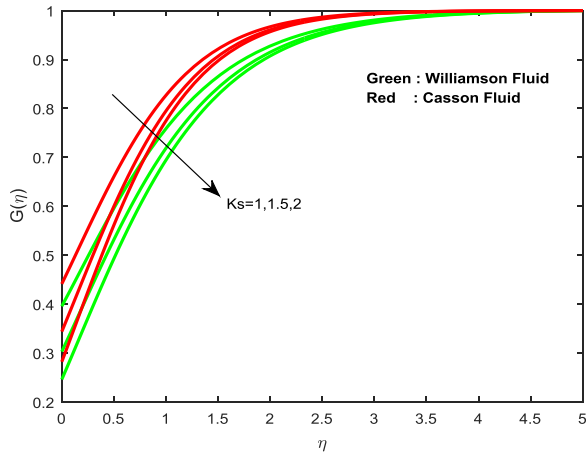


**Fig.7** Concentration field for different values of heterogeneous parameter

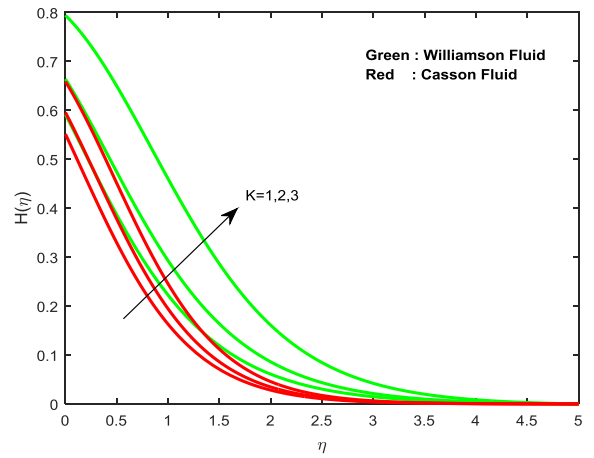


**Fig.10** Concentration field for different values of homogeneous parameter

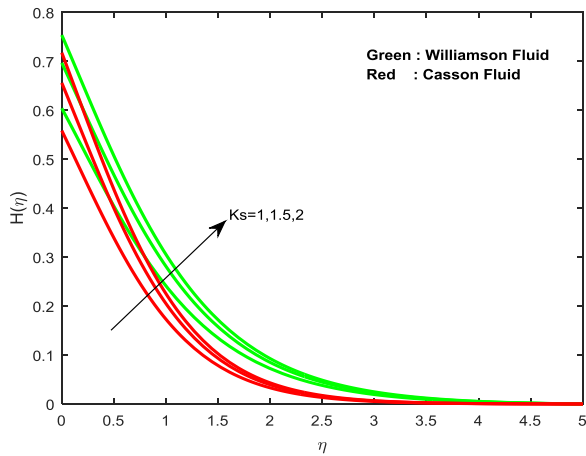


**Fig.8** Concentration field for different values of heterogeneous parameter

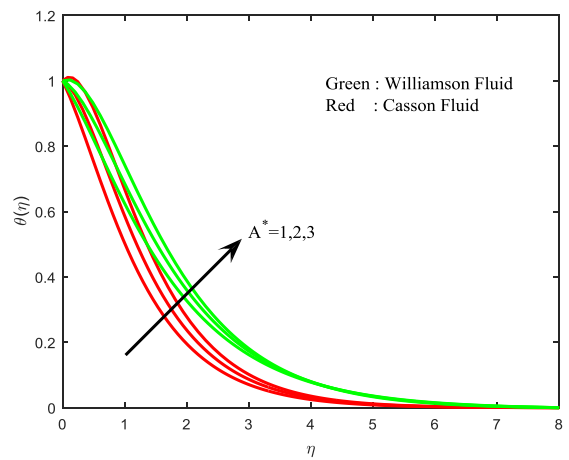


**Fig.11** Temperature field for different values of non-uniform heat source/sink

**Fig.12 Temperature field for different values of non-uniform heat source/sink**

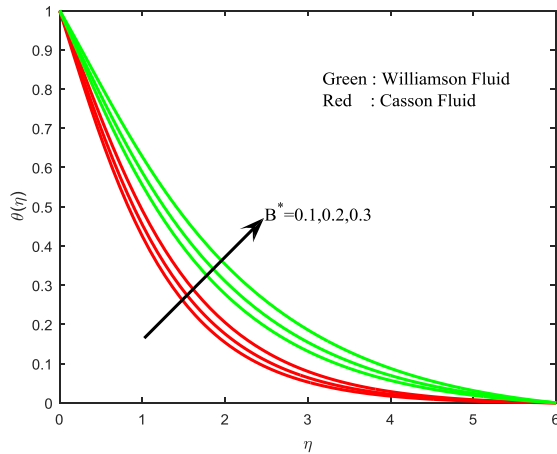


**Table 2 Variation in local Nusselt number for different non-dimensional parameters**

$M$	$A^*$	$B^*$	$\Lambda$	Williamsons Fluid	Casson Fluid
				$-\theta'(0)$	$-\theta'(0)$
1				1.061980	1.168202
2				1.018127	1.138109
3				0.979309	1.111184
	1			1.112722	1.202743
	1.5			1.037060	1.122265
	2			0.961398	1.041787
		1		1.112722	1.202743
		2		0.932339	1.052899
		3		0.702747	0.878507
			1	1.086327	1.184807
			2	1.039332	1.152696
			3	0.998170	1.124307

**Table 3 Variation in mass transfer rates for different non-dimensional parameters**

$M$	$K_s$	$K$	Williamsons Fluid	Casson Fluid	Williamsons Fluid	Casson Fluid
			$-G'(0)$	$-H'(0)$	$-G'(0)$	$-H'(0)$
1			-0.383716	-0.616284	-0.434633	-0.565367
2			-0.360601	-0.639399	-0.421729	-0.578271
3			-0.338536	-0.661464	-0.409593	-0.590407
	1		-0.395795	-0.604205	-0.441462	-0.558538
	1.5		-0.454525	-0.696983	-0.515960	-0.656027
	2		-0.492470	-0.753765	-0.564671	-0.717664

		1	-0.408322	-0.591678	-0.448612	-0.551388
		2	-0.336087	-0.663913	-0.404352	-0.595648
		3	-0.205770	-0.794230	-0.341113	-0.658887

**Table 4 Comparison of the values of  $\left(1 + \frac{1}{\beta}\right) f''(0)$  when  $K = K_s = A^* = B^* = 0$**

$M$	$\Lambda$	$\beta$	Ahmad and Nazar [30]	Present Results
0	0	$\infty$	-1.0042	-1.00421
0	0	5	-1.0954	-1.09542
0	0.5	1	-1.7320	-1.73200
10	0	$\infty$	-3.3165	-3.31653
10	0	5	-3.6331	-3.63311
10	0.5	1	-4.7958	-4.79582

## 6. Conclusions

The Casson fluid as well as Williamson fluids have specific importance in industrial as well as biomechanical engineering fields. The main motivation of this study due to importance of automatic system (Casson and Williamson fluids are small variation in viscosity) presented a numerical solution to analyze the heat and mass transfer production in MHD Casson and Williamson fluids past a stretching surface in the presence of non-uniform heat source/sink and homogeneous-heterogeneous reactions. We found that the heat and mass transfer production of Casson fluid is comparatively better than the heat and mass transfer production of Williamson fluid. Momentum boundary layer thickness of Williamson fluid is effectively enhances due to variation in the non-dimensional parameters. The temperature profiles of the casson fluid are effectively enhances due to the external heat source. Homogeneous-heterogeneous parameters help to modulating the concentration boundary layer thickness. This study can be useful in automatic manufacturing and designing processes based on the viscosity nature.

## Acknowledgement

The authors extend Their appreciation to the Deanship of Scientific Research at King Saud University for funding this work through the research group project No RGP-080.

## Nomenclature

$u, v$  : Velocity components in  $x$  and  $y$  directions respectively ( $m/s$ )

$x$  : Distance along the surface ( $m$ )

$y$  : Distance normal to the surface ( $m$ )

$q_w$  : Wall heat flux ( $W/m^2$ )

$c_p$  : Specific heat capacity at constant pressure ( $J/KgK$ )

$f$  : Dimensionless velocities ( $m/s$ )  
 $T$  : Temperature of the fluid ( $K$ )  
 $q'''$  : Non uniform heat source/sink ( $K/s$ )  
 $g$  : Acceleration due to gravity ( $m/s^2$ )  
 $k_f$  : Thermal conductivity ( $W/mK$ )  
 $\alpha_f$  : Diffusion coefficient ( $m^2/s$ )  
 $\Gamma$  : Relaxation time constant  
 $u_w$  : Velocity at the wall

### Greek Symbols:

$\eta$  : Similarity variable  
 $\sigma$  : Electrical conductivity ( $S/m$ )  
 $\sigma^*$  : Stefan-Boltzmann constant ( $W/m^2K^4$ )  
 $k^*$  : Mean absorption coefficient  
 $\theta$  : Dimensionless temperature ( $K^0$ )  
 $\rho$  : Density of the fluid ( $Kg/m^3$ )  
 $\nu_f$  : Kinematic viscosity ( $m^2/s$ )  
 $\mu$  : Dynamic viscosity of the fluid ( $Kg/ms$ )  
 $\phi$  : Nanoparticle volume fraction  
 $\mu_\infty$  : Viscosity of the ambient fluid  
 $T_w, T_\infty$  : Temperatures of the near and far away from the surface  
 $c, d$  : The constant parameters  
 $a, b$  : The concentration of the chemical species  
 $k_c, k_s$  : The rate constants  
 $D_A, D_B$  : Diffusion coefficients

### Dimensional less parameters:

$A^*, B^*$  : Non-uniform heat generation/absorption coefficient  
 $Cf_x$  : Skin friction coefficient in  $x$ -direction  
 $Cf_y$  : Skin friction coefficient in  $y$ -direction  
 $Nu_x$  : Local Nusselt number  
 $Sh_x$  : Local Sherwood number  
 $Sc$  : Schmidt number  
 $K$  : Strength of homogeneous parameter

$K_s$  : Strength of heterogeneous parameter  
 $\beta$  : Casson fluid parameter  
 $Re_x$  : Local Reynolds number  
 $Pr$  : Prandtl number  
 $M$  : Magnetic field parameter  
 $\lambda$  : Non-Newtonian fluid parameter  
 $\delta$  : The ratio of diffusion coefficient  
 $G$  : Strength of homogeneous concentration  
 $H$  : Strength of heterogeneous concentration

### Subscripts:

$f$  : Fluid  
 $w$  : Condition at the wall  
 $\infty$  : Condition at the free stream

### References

- [1]. Sakiadis, B. C., Boundary layer behavior on continuous solid surface: Boundary layer equations for two-dimensional and axisymmetric flow, *J. Amer. Inst. Chem. Eng.* 7 (1961), pp. 26-28.
- [2]. Ali, M. E., Al-Yousef, F., Laminar mixed convection from a continuously moving vertical surface with suction or injection, *Heat and Mass Transfer* 33 (1998), 4, pp. 301-306, 1998.
- [3]. Magyari, E., Ali, M. E., Keller, B., Heat and mass transfer characteristics of the self-similar boundary-layer flows induced by continuous surfaces stretched with rapidly decreasing velocities, *Heat and Mass Transfer* 38, (2001) ,(1-2), pp. 65-74.
- [4]. Chamka, A. J., MHD flow of a uniformly stretched vertical permeable surface in the presence of heat generation/absorption and a chemical reaction, *Int. Comm. Heat Mass Trans.* 30 (2003), pp. 413-422.
- [5]. Raptis, A., Perdakis, C., Viscous flow over a non-linearly stretching sheet in the presence of a chemical reaction and magnetic field, *Int. J. Non-linear Mech.* 41 (2006), pp. 527-529.
- [6]. P. M. Patil, P. S. Kulkarni, Effects of chemical reaction on free convective flow of a polar fluid through a porous medium in the presence of internal heat generation, *Int. J. Thermal Sci.* 47 (2008), pp. 1043-1054.
- [7]. Ali, M. E., The effect of variable viscosity on mixed convection heat transfer along a vertical moving surface, *Int. J. of Thermal Science*, 45 (2006),1 pp. 60-69.
- [8]. Cortell, R., MHD flow and mass transfer of an electrically conducting fluid of second grade in a porous medium over a stretching sheet with chemically reactive species, *Chemical Engineering and Processing*, 46 (2007) pp. 721-728.
- [9]. Raju, C. S. K., N. Sandeep, and S. Saleem. Effects of induced magnetic field and homogeneous–heterogeneous reactions on stagnation flow of a Casson fluid. *Engineering Science and Technology, an International Journal* 19.2 (2016) 875-887.
- [10]. Haq, R. U., Nadeem, S., Khan, Z. H., Okedayo, T. G., Convective heat transfer and MHD effects on casson nanofluid flow over a shrinking sheet, *Cent. Eur. J. Phys.* 12 (2014), pp. 862-871.

- [11]. A. Hussain, M. Z. Salleh, R. M. Tahar, I. Khan, Unsteady boundary layer flow and heat transfer of a casson fluid past an oscillating vertical plate with Newtonian heating, *Plos One* 9 (2014), pp. e108763.
- [12]. Raju, C. S. K., Sandeep, N., Sugunamma, V., Jayachandrababu, M., Ramanareddy, J. V., Heat and mass transfer in magneto hydrodynamic casson fluid over an exponentially permeable stretching surface, *Eng. Sci. Tech., an Int. J.*, (2015), <http://dx.doi.org/10.1016/j.jestch.2015.05.010>.
- [13]. Nadeem, S., Haq, R. U., Lee, C., MHD flow of a casson fluid over an exponentially shrinking sheet, *Scientia Iranica B* 19 (2012), pp. 1550-1553.
- [14]. Nadeem, S., Haq, R. U., Akbar, N. S., Khan, Z. H., MHD three-dimensional casson fluid flow past a porous linearly stretching sheet, *Alexandria Engineering J.* 52 (2013), pp. 577-582.
- [15]. Ramzan, M., Farooq, M., Alsaedi, A., Hayat, T., MHD three-dimensional flow of couple stress fluid with Newtonian heating, *Eur. Phys. J. Plus* 49 (2013), pp. 128.
- [16]. Hayat, T., Shehzad, S. A., Alsaedi, A., Three-dimensional stretched flow of Jeffrey fluid with variable thermal conductivity and thermal radiation, *Applied Mathematics and Mech.* 34 (2013), pp. 823-832.
- [17]. Ali, M. E., The buoyancy effects on the boundary layers induced by continuous surfaces stretched with rapidly decreasing velocities, *Heat and Mass Transfer* 40 (2004), (3-4), pp. 285-291.
- [18]. Mahantha, G., Shaw, S., 3D Casson fluid flow past a porous linearly stretching sheet with convective boundary condition, *Alexandria Eng. J.* 54 (2015), pp. 653-659.
- [19]. Sandeep, N., Raju, C. S. K., Sulochana, C., Sugunamma, V., Effects of aligned magnetic field and radiation on the flow of ferrofluids over a flat plate with non-uniform heat source/sink, *Int. J. Sci. Eng.* 8 (2015), pp. 151-158.
- [20]. Hayat, T., Saeed, Y., Asad, S., Alsaedi, A., Soret and dufour effects in the flow of Williamson fluid over an unsteady stretching surface with thermal radiation, *Z. Naturforsch.* 70 (2015), pp. 235-243.
- [21]. Khan, N. A., Khan, S., Riaz, F., Boundary layer flow of Williamson fluid with chemically reactive species using scaling transformation and homotopy analysis method, *Math. Sci. Lett.* 3 (2014), pp. 199-205.
- [22]. Hayat, T., Abbas, Z., Sajid, M., Heat and mass transfer analysis on the flow of a second grade fluid in the presence of chemical reaction, *Physics Letters A*, 372 (2008), (14), pp. 2400-2408.
- [23]. Annimasun, I. L., Raju, C. S. K., Sandeep, N., Unequal diffusivities case of homogeneous-heterogeneous reactions within viscoelastic fluid flow in the presence of induced magnetic field and nonlinear thermal radiation, *Alexandria Engineering journal*, (2015), <http://dx.doi.org/10.1016/j.aej.2016.01.018>.
- [24]. Hayat, T., Tanveer, A., Yasmin, H., Alsaedi, A., Homogeneous-heterogeneous reactions in peristaltic flow with convective conditions, *Plos one* 9 (2014), pp. e113851.
- [25]. Bachok, N., Ishak, A., Pop, I., On the stagnation point flow towards a stretching sheet with homogeneous-heterogeneous reactions effects, *Commun. Nonlinear Sci. Numer. Simul.* 16 (2011), pp. 4296-4302.
- [26]. Chatterjee, A., Heat transfer enhancement in laminar impinging flows with a non-Newtonian inelastic fluid, *J. Non Newtonian Fluid Mech.* 211 (2014), pp. 50-61.
- [27]. Delenda, N., Hirata, S. C., Ouarzazi, M. N., Primary and secondary instabilities of viscoelastic mixtures saturating a porous medium: Application to separation of species, *J. Non Newtonian Fluid Mech.* 181-182 (2012), pp. 11-21.
- [28]. Sandeep, N., Sulochana, C. Dual solution for unsteady mixed convection flow of MHD Micropolar fluid over a stretching/shrinking sheet with non-uniform heat source/sink, *Engineering Science and Technology, an International Journal*, 18(2015), pp. 1-8.

- [29]. Chaudhary, M. A., Merkin, J. H., A simple isothermal model for homogeneous-heterogeneous reactions in boundary layer flow: I. Equal Diffusivities, *Fluid Dynamics Res.* 16 (1995), pp. 311-333.
- [30]. Ahmad, K., Nazar, R., Magnetohydrodynamic three-dimensional flow and heat transfer over a stretching surface in a viscoelastic fluid, *J. Science and Technology* 3 (2011), pp. 33-46.
- [31]. Ramesh, G. K., B. J. Gireesh, and C. S. Bagewadi. "Heat Transfer in MHD Dusty Boundary Layer flow of over an inclined stretching surface with non-uniform heat source/sink, *Advances in Mathematical Physics*, volume-Article ID 657805 (2012) 13.
- [32]. Awais, M., Saleem, S., Hayat, T., & Irum, S. (2016). Hydromagnetic couple-stress nanofluid flow over a moving convective wall: OHAM analysis. *Acta Astronautica*, 129, 271-276.
- [33]. Ramesh G.K., Numerical study of the influence of heat source on stagnation point flow towards a stretching surface of a Jeffrey fluid nanoliquid, *Journal of Engineering*, Volume 2015, Article ID: 382061.
- [34]. Nadeem, S., and S. Saleem. Analytical study of third grade fluid over a rotating vertical cone in the presence of nanoparticles. *International Journal of Heat and Mass Transfer* 85 (2015) 1041-1048.
- [35]. Ramesh, G. K., Ali J. Chamkha, and B. J. Gireesha. MHD mixed convection flow of a viscoelastic fluid over an inclined surface with a nonuniform heat source/sink. *Canadian Journal of Physics* 91.12 (2013) 1074-1080.
- [36]. Saleem, Salman, Sohail Nadeem, and Muhammad Awais. Time-Dependent Second-Order Viscoelastic Fluid Flow on Rotating Cone with Heat Generation and Chemical Reaction. *Journal of Aerospace Engineering* 29.4 (2016) 04016009.
- [37]. Awais, M., Hayat, T., Irum, S., & Saleem, S. (2015). Dual Solutions for Nonlinear Flow Using Lie Group Analysis. *PloS one*, 10(11), e0142732.
- [38]. Nadeem, S., Z. Ahmed, and S. Saleem. The Effect of Variable Viscosities on Micro polar Flow of Two Nanofluids. *Zeitschrift für Naturforschung A* 71.12 (2016) 1121-1129.
- [39]. Raju, C. S. K., and N. Sandeep, Unsteady three-dimensional flow of Casson–Carreau fluids past a stretching surface. *Alexandria Engineering Journal* 55(2) (2016) 1115-1126.
- [40]. Nadeem, S, S. T. Hussain, C. Lee, Flow of Williamson fluid over a stretching sheet, *Brazilian Journal Chemical Engineering*, 30 (2013) 619-625.

Submitted: 26.04.2016.  
 Revised: 03.04.2017.  
 Accepted: 05.04.2017.